Evidence of recent active volcanism in the Balleny Islands (Antarctica) from ice core records

Dieter. R. Tetzner[1,2], Elizabeth. R. Thomas[1], Claire. S. Allen[1] and Alma. Piermattei[3]

[1]British Antarctic Survey, Cambridge, United Kingdom. [2]Department of Earth Sciences, University of Cambridge, Cambridge, United Kingdom. [3]Department of Geography, University of Cambridge, Cambridge, United Kigdom.

Corresponding author: Dieter Tetzner (dietet95@bas.ac.uk)

Key Points:

- Evidence of active volcanism in the sub-Antarctic Balleny Islands in 2001 AD, supporting un-verified images from satellites.
- The identification of a 21st century volcanic chronostratigraphic marker in ice cores from the Antarctic Peninsula and West Antarctica.

Abstract

Records of active volcanism in Antarctica provide key information to understand the role of volcanoes shaping the polar climate and its potential impacts on the cryosphere. The lack of historical records of volcanic activity in the region has limited our comprehension of Antarctic volcanism. Remote sensing can provide insight into active volcanism during the satellite era, although the evidence is often inconclusive. Here we present a detailed study from multiple Antarctic ice cores to provide independent evidence of active volcanism in the sub-Antarctic Balleny Islands in 2001 AD, supporting un-verified images from satellites. The ice core records reveal elevated inputs of sulphate and microparticles from a local Antarctic volcanic source. In-phase deposition of volcanic products confirmed a rapid tropospheric transport of volcanic emissions from a small-to-moderate, local eruption during 2001. Air mass trajectories demonstrated some air parcels were transported over the West Antarctic Ice sheet from the Balleny Islands to ice core sites at the time of the potential eruption, establishing a route for transport and deposition of volcanic products over the ice sheet. The data presented here validate previous remote sensing observations and confirms a volcanic event in the Balleny Islands during 2001 AD. This newly identified eruption provides a case study of recent Antarctic volcanism and a consistent XXI century chronostratigraphic marker for ice core sites in Marie Byrd Land, Ellsworth Land and the southern Antarctic Peninsula.

1 Introduction

Antarctica is one of the least volcanically active regions in the world, with the highest number of volcanoes listed as uncertainly active and many others hidden beneath the ice sheet (Hund, 2014). Over 100 volcanoes have been identified in the Antarctic continent and sub-Antarctic Islands (LeMasurier et al., 1990; de Vries et al., 2018) with more than twenty documented in the historical records (Patrick & Smellie, 2013). Among the historically active, just two are frequently monitored by ground-based instruments (Mount Erebus and Deception Island) (LeMasurier et al., 1990; Patrick & Smellie, 2013), while the others are rarely surveyed due to their extreme isolation. Recently, remote sensing techniques have helped to monitor volcanism through the region. However, high detection thresholds and coarse spatial resolution have hindered the capacity of some sensors to identify accurately the occurrence of volcanic activity (Patrick & Smellie, 2013). Moreover, the effects of volcanism can be rapidly obscured in the Antarctic and sub-Antarctic environment due to frequent snowfall and cloud coverage (LeMasurier et al., 1990). Even though Antarctic volcanoes do not present significant direct hazards, their study is important for many areas of research. Mainly, geothermal heat flux estimates (Vogel et al., 2006), ice flow dynamics models (Bingham & Siegert 2009) and the volcanic effects on the polar climate (Robock, 2000; Cole-Dai, 2010; Sigl et al., 2014). Altogether, the remoteness and inaccessibility of most of the Antarctic volcanoes have strongly limited our knowledge of the Antarctic volcanic activity.

An alternative way to study volcanic activity in Antarctica is the analyses of volcanic tephra (assortment of fragments, from blocks of material to ash, ejected into the air during a volcanic eruption) (Kittleman, 1979) preserved in ice core layers. Volcanic eruptions emit large amounts of particulate matter and sulphur compounds into the atmosphere. Sulphur compounds are oxidized to sulphuric acid ($H_2SO_4^{2-}$) and travel as particulate aerosols in the atmosphere. Volcanic sulphate aerosols and tephra in the atmosphere can be transported thousands of

kilometres from the volcanic source, to be deposited and preserved on polar ice sheets (Koffman et al., 2017). Measurements of sulphate concentrations and electric conductivity (EC) in the ice strata help to detect and quantify past volcanic activity over thousands of years (Cole-Dai et al., 1997; Cole-Dai, 2010). Similarly, the physical and chemical characterization of tephra and cryptotephra (micrometre-sized tephra) embedded in ice layers can record past volcanic activity and fingerprint the source of the volcanic eruptions (Dunbar & Kurbatov, 2011; Narcisi et al., 2019). These methods have been applied to several Antarctic ice cores, providing evidence of past volcanic activity at regional, hemispheric and global scales (Udisti et al., 2000; Basile et al., 2001; Jiang et al., 2012; Parrenin et al., 2012; Severi et al., 2012; Fujita et al., 2015; Narcisi et al., 2016; Lee et al., 2019). From a regional perspective, the study of volcanic products preserved in ice cores has contributed to determining the recurrence of explosive volcanic activity in different volcanic groups and provinces around Antarctica (Narcisi et al., 2005; Narcisi et al., 2010; Narcisi et al., 2012).

Previous studies have demonstrated that ice cores from the Antarctic Peninsula, Ellsworth Land and Marie Byrd Land record large-scale and regional explosive volcanic eruptions (Palais, 1985; Cole-Dai et al., 1997; Dunbar et al., 2003; Dixon et al., 2004; Dunbar & Kurbatov, 2011; Abram et al., 2011; Mulvaney et al., 2012; Koffman et al., 2013; Goodwin, 2013; Thomas & Abram, 2016). Most studies have focused on detecting large explosive tropical eruptions (Pinatubo (1991), Agung (1963), Tambora (1815), among others) to establish absolute time markers for ice core chronologies or set tie-points to synchronize different records. Only a few studies document regional volcanism, mostly focused on volcanic activity in Deception Island, off the northern Antarctic Peninsula (Aristarain & Delmas, 1998; Jiankang et al., 1999; Dunbar et al., 2003; Mulvaney et al., 2012; Koffman et al., 2013).

The Balleny Islands are a chain of volcanic islands off the coast of Victoria Land, Antarctica. Sturge Island (1167 m a.s.l) is the largest and southernmost island in the volcanic chain (LeMasurier et al., 1990). This island is a stratovolcano covered by an icecap with no records of present or past volcanic activity (Hund, 2014). On 12th of June 2001 (1352 UTC), an unusual cloud formation was spotted over Sturge Island by the U.S. National Ice Center using Optical Line Scan Imagery and was still visible, attached to the island, on MODIS imagery at 2245 UTC. Satellite imagery analyses determined the cloud was a single feature in the region, reaching a visible extension of 300 km downwind (E-NE), with a maximum cloud top at approximately 6 km and revealed the possible presence of volcanic SO_2. However, the same analyses revealed the absence of ash in the cloud, presenting the satellite imagery data alone as inconclusive to determine if the cloud was produced by a volcanic eruption in Sturge Island (Global Volcanism Program, 2001).

Here we present a detailed study of five ice core glaciochemical and microparticle records from the southern Antarctic Peninsula, Ellsworth Land and Marie Byrd Land, to validate the occurrence of recent active volcanism in the Balleny Islands. Forward air mass trajectories are used to track the air masses originating from the Balleny Islands at the time of the potential 2001 eruption. Additionally, we include the analysis of insoluble particle matter in the ice cores and explore the presence of cryptotephra as absolute markers of volcanic activity. The aim of this study is to provide independent ice core evidence for a 2001 volcanic eruption on Sturge Island and present a potential absolute age-marker for Antarctic ice core chronologies.

2 Methods

2.1 Study sites

Five ice cores from the southern Antarctic Peninsula, Ellsworth Land and Marie Byrd Land were included in this study (Figure 1) (Table 1). The cores were selected due to their downwind location from the Balleny Islands, their retrieval after the 2001 austral winter, their temporal resolution (>10 samples in the youngest year), their regional distribution and their data availability. Among the five ice cores used in this study, four (GOM, BC, 01-4, WAIS) have been previously published (Table 1). The 140 m Jurassic ice core (JUR) was drilled by the British Antarctic Survey on the English Coast, Southern Antarctic Peninsula during the austral summer 2012/2013. Ice core samples were cut using a band−saw with a steel blade and then melted using a Continuous Flow Analysis (CFA) system (Rothlisberger et al., 2000) in the ice chemistry lab at the British Antarctic Survey, UK. An ice core chronology was established based on the hydrogen peroxide annual cycle that is assumed to peak during the summer solstice. The top 53.5 m included in this work were dated back to 1977 AD, with an estimated dating error for the 1977-2013 interval of ±3 months for each year and with no accumulated error. Discrete ice core samples were cut at 5 cm resolution for major ion analysis (including Methanesulphonic Acid (MSA), sodium and sulphate) with ion chromatography, using a reagent−free Dionex ICS−2500 anion and IC 2000 cation system.

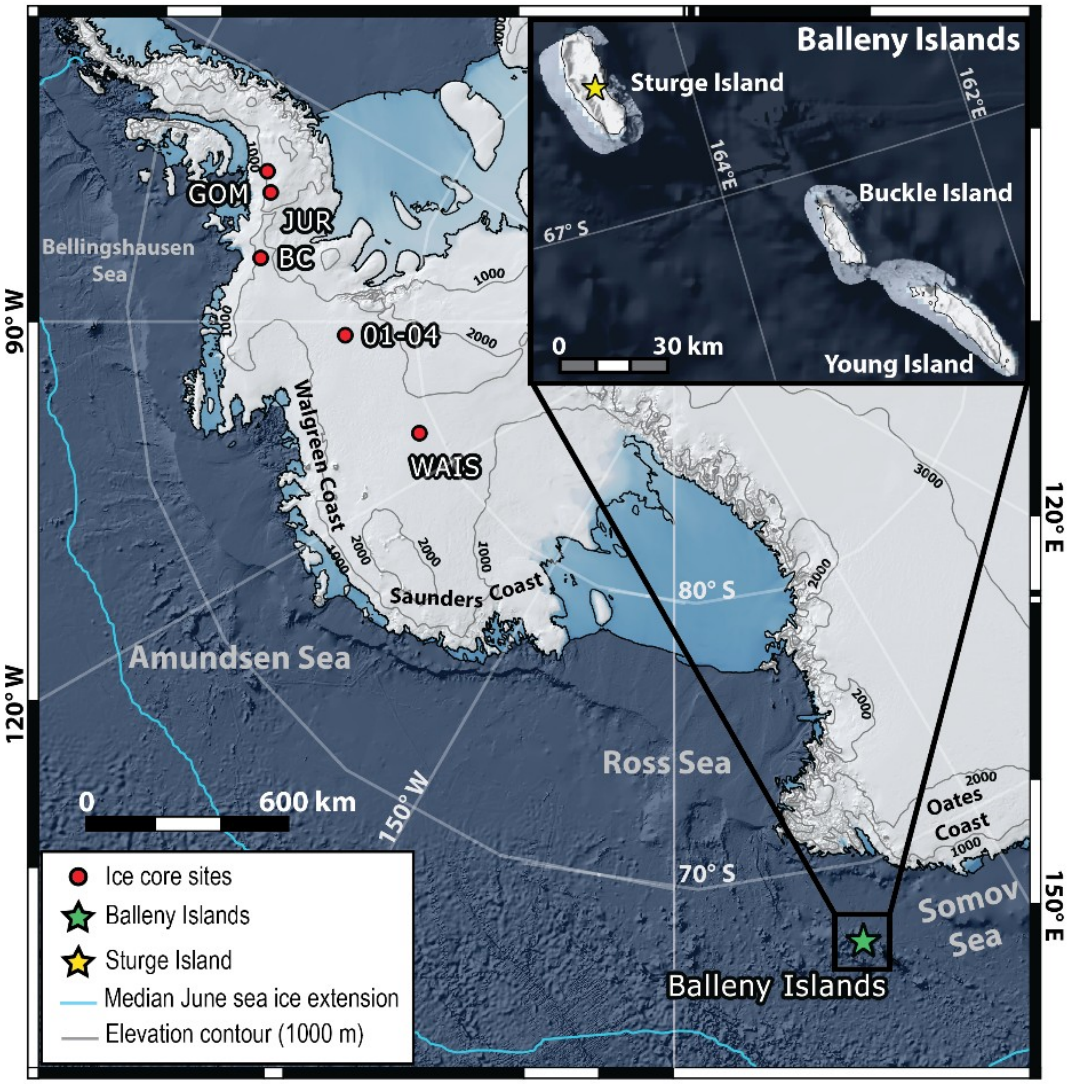

Figure 1. Map showing the ice core sites considered in this study. The red circles show the locations of the five ice core sites. The yellow star shows the location of Sturge Island in the Balleny Islands (green star). The light blue line shows the median June sea ice-extension between 1980-2010 AD

Four ice cores (GOM, JUR, BC and WAIS) were evaluated over a 30-year overlapping period (1977-2007 AD) for evidence of a volcanic eruption in the 2001 ice layer (hereafter referred to as 2001L) The ITASE 01-4 ice core, drilled in 2002, was evaluated over a 25-year overlapping period (1977-2002 AD). Additionally, two previously identified ice core horizons were targeted as examples of well-dated recent volcanic events recorded in ice core layers. The 1994-1992 AD horizon for the Mount Pinatubo and Cerro Hudson eruption (Pinatubo/Hudson) (1991 AD) (Cole-Dai & Mosley-Thompson, 1999; Zhang et al., 2002; Jiang et al., 2012; Plummer et al., 2012; Osipov et al., 2014; Schwanck et al., 2017; Thoen et al., 2018; Hoffmann et al., 2020) and the 1984-1982 AD horizon for the El Chichón eruption (1982 AD) (Traufetter et al., 2004; Jiang et al., 2012; Plummer et al., 2012; Thoen et al., 2018). Both eruptions are observed in younger ice core horizons because of the lagged deposition of volcanic sulphates

over the Antarctic ice sheet after large low-latitude eruptions (Cole-Dai et al., 1997). All ages presented in this work are based on the ice chronologies reported for each core (Table1).

Table 1. Summary of each ice core geographical location and main features of the datasets analysed in this study. Abbr: Abbreviation.

Core Name	Abbr.	Long	Lat	Elevation (m a.s.l.)	Year drilled (AD)	Depth interval (m)	Sample resolution (m)	Ice chronology
Gomez	GOM	-70.36	-73.59	1400	2007	0-45.48	0.02	Thomas et al., 2008
Jurassic	JUR	-73.06	-74.33	1139	2013	10.14-53.5	0.05	This work
Bryan Coast	BC	-81.67	-74.49	1177	2011	4.41-28.45	0.05	Thomas et al., 2015
ITASE 01-4	01-4	-92.25	-77.61	1483	2002	0-16.56	0.03	Mayewski & Dixon, 2005
WAIS Divide	WAIS	-112.09	-79.47	1797	2007	0-12.50	0.03	Sigl et al. 2016

2.2 Sulphate concentration analyses

Sulphate from volcanic eruptions is superimposed over the background sulphate. This includes organic sulphur compounds, such as dimethyl sulphide (DMS), from marine biogenic emissions (Maupetit & Delmas, 1992; Cole-Dai et al., 2000; Castellano et al., 2004; Dixon et al., 2004; Nardin et al., 2020), with a smaller contribution from sea salt aerosols. Even though the background sulphate is temporally variable, it can be assumed as relatively constant in the last centuries (Kreutz et al., 1999; Kreutz et al., 2000; Traversi et al., 2002; Castellano et al., 2004). Therefore, for the detection of volcanic signals, it is crucial that the correct assessment of the background sulphate concentration, and its variability is established. In particular, the accurate detection of small and moderate volcanic events depends on how the background sulphate is quantified and the volcanic detection threshold established (Cole-Dai et al., 1997; Budner & Cole-Dai, 2003; Castellano et al., 2004). Several methods have been proposed (Cole-Dai et al., 1997; Castellano et al., 2004; Traufetter et al., 2004; Gautier et al 2016) based on the evaluation of a background sulphate representative value (m) and its standard deviation (σ) to establish a threshold (m+2σ). Sulphate peaks above this threshold are considered indicative of volcanic activity.

In this work, the background signal is evaluated in the total sulphate concentration (SO_4^{2-}) and in the non-sea salt sulphate flux ($nssSO_4^{2-}$-flux) (Cole-Dai et al., 1997). The $nssSO_4^{2-}$-flux was calculated using Equation 1 and Equation 2 (Wagenbach et al., 1998), and using sodium (Na^+) as the reference ion (Castellano et al., 2004; Dixon et al., 2004; Ren et al., 2010; Li et al., 2012; Jiang et al., 2012; Osipov et al., 2014). The analysis of the $nssSO_4^{2-}$-flux was incorporated because it facilitates the detection of small and moderate volcanic signals (Cole-Dai et al., 1997; Zhang et al., 2002). In the absence of sulphate data from the GOM ice core, the total sulphur (S_{tot}) and non-sea salt sulphur flux (nssS-flux) were used for calculations.

¿ (Equation 1)

$nssSO_4^{2-}{}_{¿flux=¿¿}$ (Equation 2)

To detect volcanic eruptions from elevated SO_4^{2-} and $nssSO_4^{2-}$-flux, we applied the method originally proposed by Castellano et al. (2004). This method was selected over other methods (Cole-Dai et al., 1997; Traufetter et al., 2004) because it considers the lognormal distribution of the sulphate data. The use of lognormal statistics in sulphate analyses has been proven to clearly differentiate between volcanic sulphate and background sulphate (Castellano et al., 2004). To calculate the background sulphate, new datasets were generated after excluding individual ice core horizons from well-known volcanic eruptions between 2007-1977 AD (e.g. Pinatubo/Hudson (1991 AD) and El Chichón (1982 AD)). After excluding these horizons, the background and its variability were estimated at each sample point by calculating in the log domain, the mean and standard deviation of a 20% weighted curve fit centred on each sample point (10% weighted curve fit for the shorter 01-4 ice core). To identify samples with a potential volcanic influence, the SO_4^{2-} and $nssSO_4^{2-}$flux had to exceed the background signal (m) by two times the standard deviation (>2σ-peak). This threshold ensured 95.5% of the random background variability was excluded. SO_4^{2-} and $nssSO_4^{2-}$flux>2σ-peaks were classified based on the number of data points exceeding the threshold (single point (=1) or multiple points (>1)). The method applied in this study assumes that in the absence of inputs from large volcanic and anthropogenic sources (negligible in Antarctica), the sulphate concentration in the snow comprises inputs from regional background sulphate emissions, not controlled by a dominant source region or transport and deposition processes (Cole-Dai et al., 1997). S_{tot} and nssS-flux from GOM were analysed using the same method applied for SO_4^{2-} and $nssSO_4^{2-}$-flux volcanic detection analyses, respectively.

As previously stated, one of the main sources of background sulphate is DMS from marine biogenic emissions. The oxidation of DMS in the atmosphere produces MSA, a chemical compound widely studied in ice core records because of its link to marine biogenic emissions in the Southern Ocean (Curran et al., 2003; Abram et al., 2010; Abram et al., 2013; Criscitiello et al., 2013; Thomas et al., 2016). The MSA records available for GOM, JUR and BC ice cores are included to assess whether the SO_4^{2-}>2σ-peaks identified in the 2001L were influenced by increased marine biogenic emissions. MSA records for WAIS and 01-4 ice cores were not available.

The total Na^+ concentration in ice is largely determined by the interaction of airmasses with marine open waters and potential short-term inputs from volcanic ash (Legrand & Mayewski, 1997). Since the $nssSO_4^{2-}$-flux is calculated using Na^+ as the reference ion, it is crucial to study the variability of SO_4^{2-} and Na^+. The Na^+ record from each of the five ice cores was included to assess whether the $nssSO_4^{2-}$-flux values in the 2001L were influenced by additional inputs from non-volcanic sources.

Volcanic sulphate fluxes were calculated for two of the targeted periods (2001L and 1992-1994 AD). The 1984-1982 AD horizon for the El Chichón eruption (1982 AD) was not included due to the lack of >2σ-peaks in the $nssSO_4^{2-}$flux profiles. To calculate the volcanic sulphate flux, the background $nssSO_4^{2-}$-flux was subtracted from the sample $nssSO_4^{2-}$-flux on each volcanic event identified (>2σ-peak). Therefore, the total flux for a volcanic event is the sum of all the residuals of $nssSO_4^{2-}$-flux samples from the corresponding layers and over the background $nssSO_4^{2-}$-flux (Jiang et al., 2012). Where elevated $nssSO_4^{2-}$-flux does not exceed the detection threshold (m+2σ), the volcanic sulphate flux was calculated as the sum of $nssSO_4^{2-}$-flux residuals within the depth interval where a SO_4^{2-}>2σ-peak was identified. To compare the 2001L volcanic sulphate fluxes among different ice cores, the 2001L $nssSO_4^{2-}$-flux was normalized

against the nssSO_4^{2-}-flux of the well-documented Pinatubo/Hudson eruption (Cole-Dai, et al., 1997). Due to the different parameters measured in GOM (S_{tot} and nssS-flux), this ice core was excluded from the volcanic sulphate flux calculations.

2.3 Physical properties analyses

The electrical conductivity (EC) signal recorded in ice is controlled by soluble impurities that originate mostly from sea salt, biomass burning, and volcanic eruptions, and is strongly correlated with acidity (Mulvaney, 2013). EC measurements from four ice cores were included in this study (only available at GOM, JUR, BC and WAIS) as an additional dataset to test the presence of volcanic products. EC was analysed in different labs using an Amber Science flow-through meter connected to a continuous ice core melter system. EC data presented a log-normal distribution. Therefore, data treatment and calculations were performed using log-normal statistics. The background conductivity, its variability and the establishment of an anomalous conductivity detection threshold were calculated following the same method presented in section 2.2 for SO_4^{2-} and nssSO_4^{2-}-flux.

2.4 Forward trajectory analyses

Forward trajectory analysis is used to examine the pathways of air masses passing over the Balleny Islands and their potential transit over the ice core sites during the deposition of the 2001L. The National Oceanic and Atmospheric Administration (NOAA)'s Hybrid Single-Particle Lagrangian Integrated Trajectory (HYSPLIT) model (Draxler & Hess, 1998; Stein et al., 2015) was used to calculate three-dimensional air parcel pathways under isobaric conditions (2.5 degree latitude-longitude resolution). Trajectories were calculated starting from the Balleny Islands for a 30-hour interval, 15 hours before and 15 hours after the first evidence of possible volcanic activity (1352 UTC on 12 June 2001). Forward trajectories were initiated every hour for up to 10 days using the NCEP/NCAR Reanalysis archives (1948 - present) with three starting elevations: 1000, 1500 and 2000 meters above the sea level (a.s.l.). These elevations were selected because of their close proximity to the summit of Sturge Island (1167 m a.s.l), from where a potential volcanic plume could have been emitted. For comparison, trajectories were classified into three groups based on their starting time relative to the first remote sensing (RS) evidence of the unusual cloud formation over Sturge Island: pre-RS evidence, firs-RS evidence and post-RS evidence.

2.5 Microparticle analyses

Microparticle Concentration (MPC) and Particle Size Distributions (PSD) were measured. Microparticle data was obtained from the JUR and WAIS ice cores. The later corresponds to the WAIS Divide deep ice core, WDC06A (Kreutz et al., 2011; Kreutz et al., 2015). MPC from the WDC06A was measured using a flow-through Klotz Abakus laser particle counter connected to a continuous ice core melter system at the University of Maine (Breton et al., 2012). Particles were measured in 31 size channels, spanning 115 μm diameter. Similarly, MPC from the JUR ice core was measured using a flow-through Klotz Abakus laser particle counter connected to a continuous ice core melter system at the British Antarctic Survey. Particles were measured in 23 size channels spanning 0.9-12 μm diameter. MPC datasets presented a log-normal distribution. Therefore, data treatment and calculations were performed using log-normal statistics. To assess whether a MPC peak in the dataset could be influenced by volcanic activity, the microparticle background concentration and its variability were calculated.

A detection threshold was set following the same guidelines presented in section 2.2 for sulphate analyses. The JUR dust record is presented with a 4-meter gap, due to problems in the data acquisition between 43.6-47.6 meters deep.

PSD were obtained by calculating the ratio of total volume of insoluble dust contained within each size bin and the derivative of the volume with respect to the natural logarithm of the particle diameter for each bin (dV/dlnD), as presented in Koffman et al. (2014). Three individual ice core horizons were targeted to characterize their PSD: The 2001 ice core horizon (2001L), Pinatubo/Hudson eruption (1991 AD) and El Chichón eruption (1982 AD). To determine if the targeted horizons differ from the background particle size of atmospheric dust, the PSD for the 1977-2007 AD period was calculated as the average PSD after removing the three targeted horizons. For PSD analyses, the mode particle diameter as a representative statistic of the volume distribution was used (Ruth et al., 2003; Koffman et al., 2014).

Microscopy analyses of microparticles were included to determine whether any of the particles present in the 2001 AD horizon were cryptotephra shards. For this, ice samples of 200 mL, from the 2001L of the JUR and GOM ice cores, were melted and filtered. Samples were melted using a Continuous Flow Analysis (CFA) system (Rothlisberger et al., 2000) in the ice chemistry lab at the British Antarctic Survey, UK. Meltwater from the CFA waste lines was collected in new bottles then filtered through 13 mm diameter, 1.0 μm pore size Whatman™ Polycarbonate membrane filters, inside clean polypropylene Swinnnex™ filter holders. Filters were mounted onto aluminium stubs for analyses on a Scanning Electron Microscope (SEM) at the Earth Sciences Department of the University of Cambridge. Filters were imaged on a Quanta-650F using Back Scattered Electrons (BSE) on a low-pressure mode. Each filter was imaged at x800 magnification for cryptotephra identification and physical characterization, following the analysis strategy presented in Tetzner et al. (2021). Two additional samples from the 2001L of the JUR ice core were melted in a class-100 clean room, then centrifuged (6 mins at 1200/1600 rpm) and decanted successively until samples were concentrated in 2–5 mL fluid. The 2–5 mL sample liquid was homogenised, pipetted onto a single coverslip (22 × 40 mm), dried in an isolated drying cupboard and then mounted onto a single microscope slide using Norland optical adhesive 61 (refractive index 1.56). Each microscope slide was scanned for the presence of cryptotephra shards.

3 Results

3.1 Geochemical analyses

3.1.1 Sulphate concentration profiles

For each core, numerous SO_4^{2-} peaks were identified (GOM (9), JUR (7), BC (6), WAIS (3) and 01-4 (14)) as exceeding the volcanic detection threshold (m+2σ) (Figure 2). The most prominent were almost exclusively associated with the target intervals with volcanic activity (2001, 1994-1992 and 1984-1982). Table 2 presents the main features for each of those peaks.

The 2001L present the most prominent SO_4^{2-}>2σ-peaks during the 1977-2007 AD period, all of them presenting an order of magnitude increase above the background. SO_4^{2-}>2σ-peaks in the 2001L are characterized either by a sharp peak during mid-2001 (GOM, JUR, BC and 01-4) or by a wide 2001/2000 austral summer peak (WAIS). The SO_4^{2-}>2σ-peaks identified within the 1994-1992 AD ice core layer are characterized by single (GOM, BC and WAIS) or multiyear

295 sulphate increases (JUR and 01-4) during the austral summer 1991/1992 AD or 1992/1993 AD.
296 SO_4^{2-}>2σ-peaks identified within the 1984-1982 AD ice core layer are consistently smaller than
297 the peaks identified in the other targeted periods and are characterized by a single increase in the
298 SO_4^{2-} concentration during the austral summer 1983/1984 AD.

299 **Table 2**. Summary of the main features of SO_4^{2-} and nssSO_4^{2-}-flux>2σ-peaks above the volcanic
300 detection threshold within the targeted periods (2001, 1992-1994, 1982-1984 AD).
301

Core	Depth interval of excess sulphate (m)	Year in ice chronology (AD)	Data points above the threshold
SO_4^{2-}			
GOM	12.16 - 12.44	2001	>1
	26.52 - 26.98	1991/1992	>1
JUR	22.30 - 22.41	2001	1
	35.64 – 36.34	1992/1993	>1
	37.19 – 37.49	1991/1992	>1
	46.90 – 47.20	1982/1983	1
BC	10.25 - 10.4	2001	>1
	18.34 - 18.54	1992/1993	1
	24.54 - 24.74	1982/1983	>1
01-4	0.56 – 0.7	2001	>1
	6.46 – 6.99	1992/1993	>1
	7.34 – 7.59	1991/1992	>1
	12.55 – 12.73	1983/1984	>1
WAIS	2.72 – 2.93	2000/2001	>1
	6.60 – 6.93	1992/1993	>1
	9.66 – 9.97	1983	1
nssSO_4^{2-}-flux			
GOM	26.52 - 26.98	1991/1992	>1
JUR	37.19 – 37.49	1991/1992	1
01-4	0.56 – 0.7	2001	>1
	6.46 – 6.99	1992/1993	>1
	12.55 – 12.73	1983/1984	>1
WAIS	2.72 – 2.93	2000/2001	1
	6.60 – 6.93	1992/1993	>1

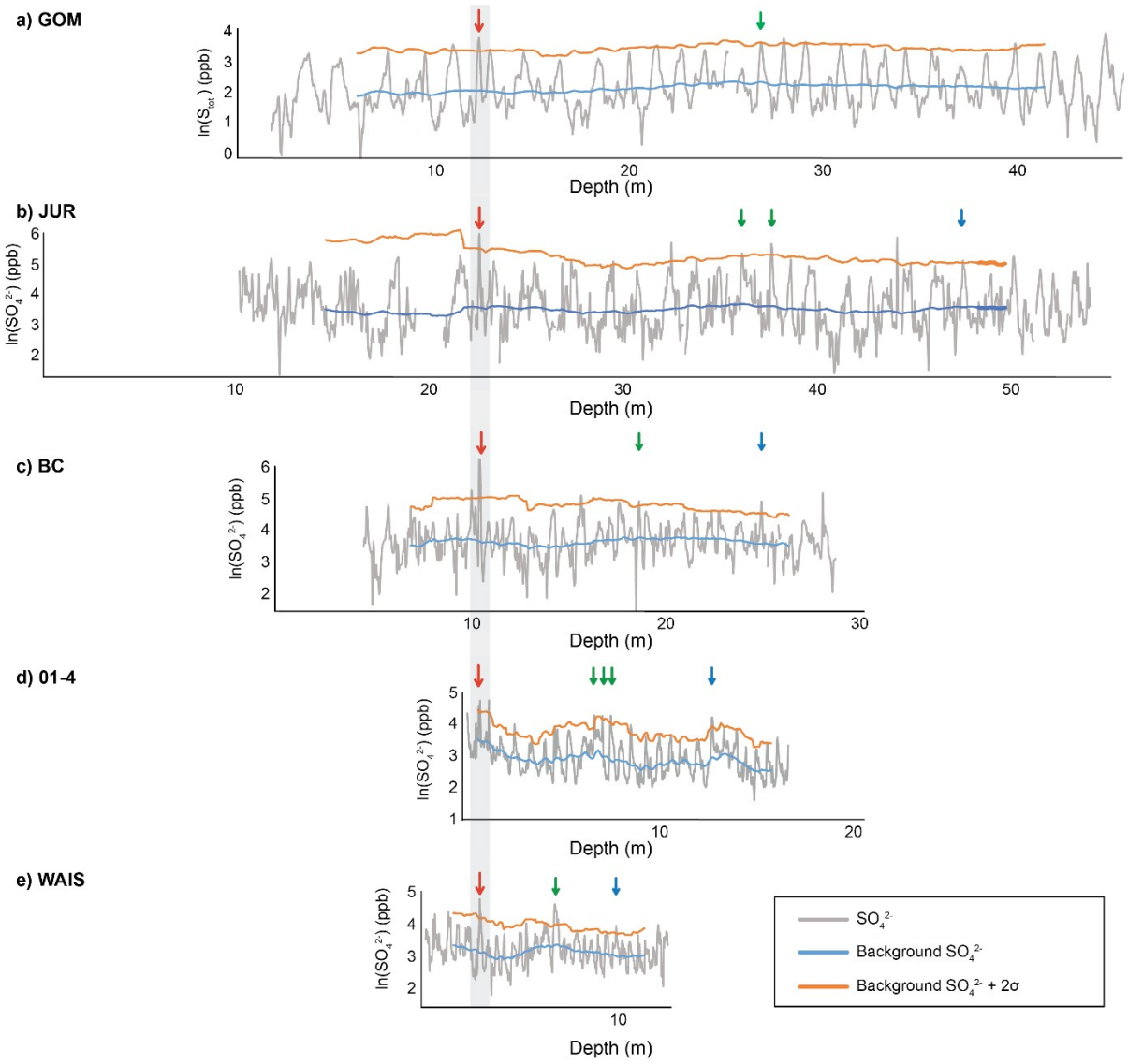

Figure 2. SO_4^{2-} profiles of the depth intervals corresponding to the 1977-2007 AD period for the five ice cores considered in this study. Arrows identify SO_4^{2-} peaks above the detection threshold (m+2σ). Red arrows indicate peaks above the detection threshold in the 2001 AD ice core layer. Green arrows indicate peaks above the detection threshold in the 1994-1992 AD ice core layer. Blue arrows indicate peaks above the detection threshold in the 1984-1982 AD ice core layer. The grey band highlights the 2001 AD ice core layer.

3.1.2 nssSO_4^{2-}-flux profiles

Twenty peaks were identified exceeding the nssSO_4^{2-}-flux volcanic detection threshold (nssSO_4^{2-}-flux>2σ): GOM (8); JUR (2); BC (1); WAIS (2) and 01-4 (7) (Figure 3). All had been previously identified as SO_4^{2-}>2σ-peaks (Figure 2). Among the nssSO_4^{2-}-flux>2σ-peaks detected, eight occurred within the targeted periods. Table 2 presents the main features for each of these eight peaks.

The most consistent and prominent $nssSO_4^{2-}$-flux>2σ-peaks were identified in the 1993-1992 AD ice core layers. The 2001L exhibited $nssSO_4^{2-}$-flux>2σ-peaks in WAIS and 01-4. The 1982-1984 AD period was represented only by a single $nssSO_4^{2-}$-flux>2σ-peak in the 01-4 core during the austral summer 1983/1984 AD.

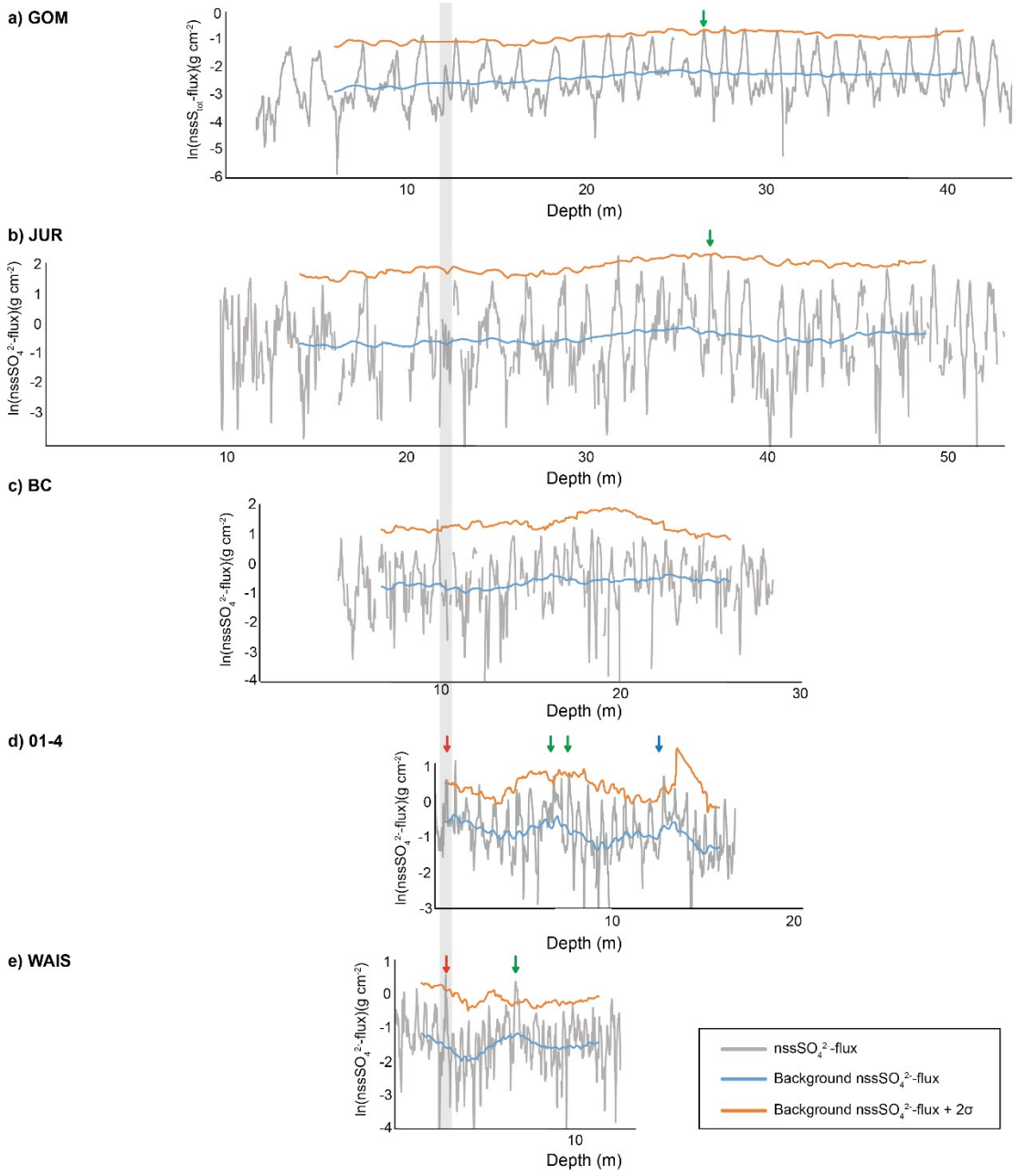

Figure 3. $nssSO_4^{2-}$-flux profiles of the depth interval corresponding to the 1977-2007 AD period for the five ice cores considered in this study. Arrows identify peaks above the detection threshold. Red arrows indicate peaks above the detection threshold in the 2001 AD ice core layer. Green arrows indicate peaks above the detection threshold in the 1994-1992 AD ice core layer. Blue arrows indicate peaks above the detection threshold in the 1984-1982 AD ice core layer. The grey band highlights the 2001 AD ice core layer.

326 3.1.2 Methanesulphonic Acid (MSA) and sodium measurements

327 MSA profiles for JUR and BC from 2001L presented prominent peaks of >35 ppb
328 indicative of spring/summer periods and a minimum <5 ppb, denoting the autumn/winter interval
329 (Figure 4). The GOM MSA profile exhibit peaks of >15 ppb indicative of spring/summer and
330 slightly smaller, isolated MSA events that correlate with autumn/winter timing e.g. at 11.71 and
331 12.20 meters deep.

332 Prominent Na^+ peaks of >1000 ppb were identified at 12.3, 10.35, and 22.36 meters deep
333 in GOM, JUR and BC, respectively (Figure 4). These peaks were more than an order of
334 magnitude above the background Na^+. Smaller increases of ~30 (ppb) in Na^+ were identified in
335 01-4 and WAIS. The 01-4 ice core presented a distinct 6-fold increase (53.15 ppb) in Na^+ over
336 the background at 0.66 meters deep. WAIS presented a minor increase of ~20 ppb in Na^+ at 2.80
337 meters deep.

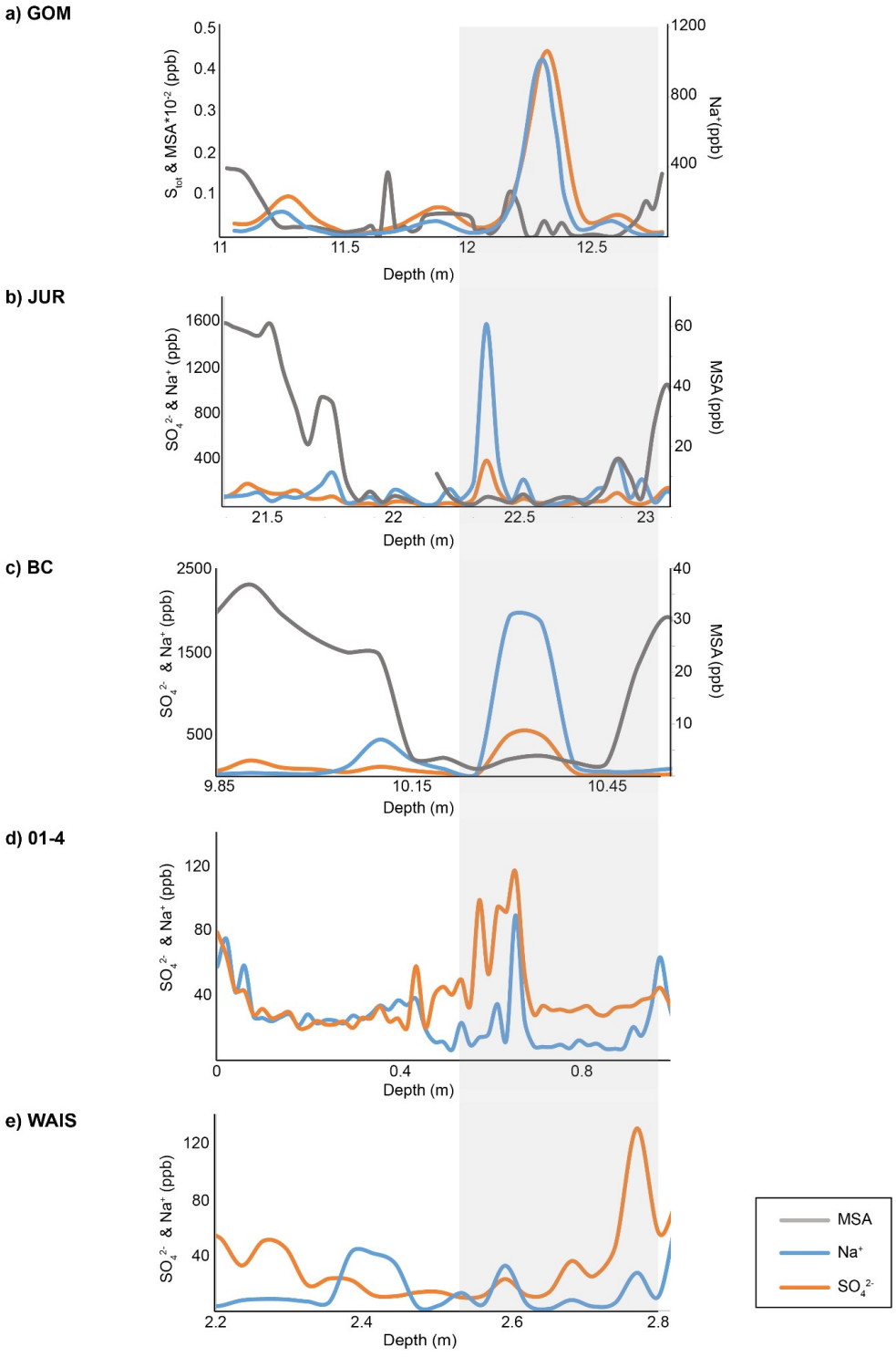

Figure 4. MSA, SO_4^{2-} and Na^+ profiles for depth interval corresponding to the 2001 AD ice core layer (2001L). The grey band highlights the January-July period in the 2001 AD ice core layer.

342 3.1.4 Volcanic sulphate flux

343 The net volcanic sulphate fluxes (VSF) for 2001L and 1993-1992 AD were calculated
344 (Table 3). The VSF ratio (2001L:1993-1992) exhibited a spatial gradient with higher values
345 (>0.42) for ice cores from Ellsworth Land-Marie Byrd Land (WAIS, O1-4) and considerably
346 lower values (<0.03) for ice cores from the southern Antarctic Peninsula (BC, JUR & GOM).

347 **Table 3**. Volcanic sulphate fluxes for the 2001 and 1993-1992 ice core layers.

Core	VSF (2001L)(g cm^{-3})	VSF (1993-1992 AD) (g cm^{-3})	VSF ratio
Jurassic	0.62	22.77	0.03
Bryan Coast	0.14	5.12	0.03
01-4	1.98	4.64	0.43
WAIS	3.77	8.13	0.46

348 3.2 Electrical conductivity (EC) profiles

349 EC profiles from four ice cores (GOM, JUR, BC and WAIS) were examined during the
350 1977-2007 AD period (Figure 5). In the GOM EC profile, eleven peaks were identified
351 exceeding the conductivity threshold (EC>2σ-peak). The most prominent identified at 12.24 m
352 (0.898 μS s^{-1}), 24.22 m (0.249 μS s^{-1}) and 34.12 m (0.335 μS s^{-1}), corresponding to years 2001,
353 1993 and 1986 AD. In the JUR EC profile, twenty-four EC>2σ-peaks were identified, with the
354 most prominent found at 18.32 m (3.21 μS s^{-1}) and 22.38 m (1.5 μS s^{-1}), corresponding to 2003
355 and 2001 AD. In the BC EC profile, fourteen EC>2σ-peaks were identified, the most prominent
356 at 10.28 m (0.701 μS s^{-1}), 15.52 m (0.385 μS s^{-1}) and 26.2 m (0.254 μS s^{-1}) corresponding to
357 2001, 1996 and 1982 AD. In the WAIS EC profile, eight EC>2σ-peaks were identified, the most
358 prominent occurring at 1.33 m (0.167 μS s^{-1}), 2.82 m (0.163 μS s^{-1}), 3.07 m (0.167 μS s^{-1}) and
359 5.36 m (0.150 μS s^{-1}), corresponding to years 2003, 2001, 2000 and 1994 AD. Three of the
360 EC>2σ-peaks were common to all four sites corresponding to years 2003, 2001 and 1994-1993.
361 The 2001 peak was among the most prominent EC>2σ-peaks in each EC profile (Figure 5).

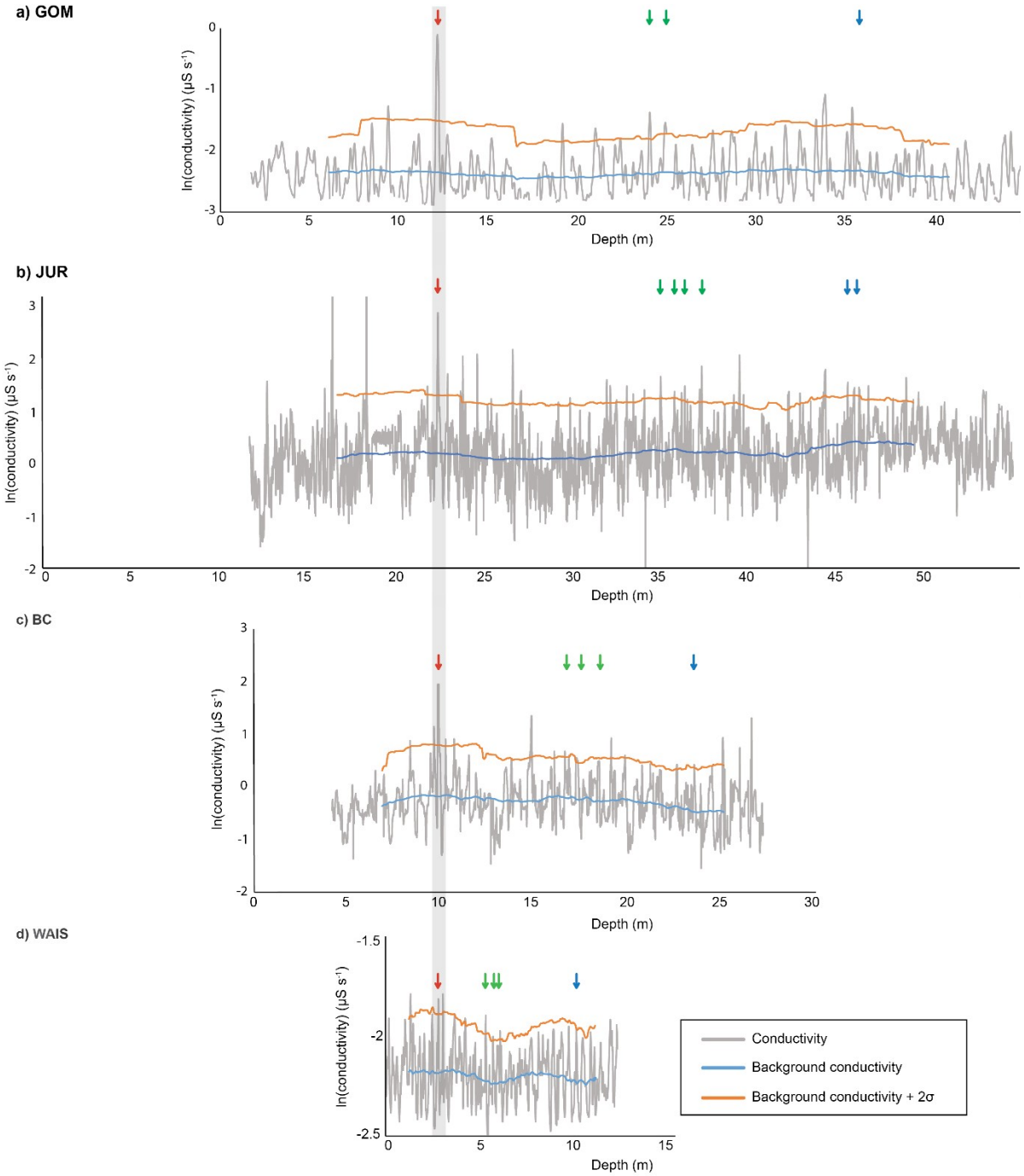

Figure 5. EC profiles for GOM, JUR, BC and WAIS for the depth interval corresponding to the 1977-2007 AD period. Red arrows indicate peaks above the detection threshold (m+2σ) in the 2001 AD ice core layer. Green arrows indicate peaks above the detection threshold in the 1994-1992 AD ice core layer. Blue arrows indicate peaks above the detection threshold in the 1984-1982 AD ice core layer. The grey band highlights the 2001 AD ice core layer.

368 ## 3.3 Microparticle analyses

369 ### 3.3.1 Microparticle concentration (MPC)

370 The MPC (particles per mL – p mL^{-1}) was examined during the 1977-2007 AD period
371 (Figure 6a and Figure 6b). In WAIS, ten peaks exceeded the MPC threshold. The most
372 prominent corresponding to the 1991-1992 AD period (6.78-6.96 m, 4257 p mL^{-1}) and smaller
373 peaks corresponding to 1982 and 2001-2000 AD (2.84 m, 2915 p mL^{-1}). In JUR, nine peaks were
374 identified. The most prominent corresponding to 1991-1992 AD (37.38 m, 6510 p mL^{-1}) with
375 smaller peaks identified corresponding to 1982 and 2001 AD.

376 ### 3.3.2 Particle size distribution (PSD)

377 The volume concentration parameter (dV/dlnD) of insoluble dust was calculated in
378 WAIS and in JUR for several particle diameters to obtain the particle size distribution (PSD)
379 (Figure 6c and 6d). In the WAIS core, the background PSD (1977-2007 AD) presented a steady
380 increase in concentration with increasing particle diameter (1.3-5.7 μm), followed by a constant
381 decrease for the coarser particles (5.7-15 μm). Similar distributions were observed in the three
382 targeted horizons, but with an additional increase in the coarsest particles (10-12 μm). Despite
383 the similarities, the PSD for Pinatubo/Hudson (1991 AD) and 2001L exhibited considerably
384 higher volume concentration values, up to four- times higher than the background, with PSDs
385 that were completely detached from the background PSD. Likewise, the PSD for El Chichón
386 exhibited higher than background volume concentration values in the finer particles (3.0-5.1
387 μm). Additional discrepancies were observed in the mode particle diameter. Whilst similar mode
388 diameters were obtained in the background (5.7 μm), Pinatubo/Hudson (5.7 μm) and El Chichón
389 (5.1 μm), the 2001L presented a considerably higher mode particle diameter (10 μm).

390 In the JUR core, the background PSD (1977-2007 AD) presented a steady increase in the
391 volume concentration with increasing particle diameter (1.0-6.0 μm), followed by a slight
392 decrease for the coarser particles (8-12 μm). The three targeted horizons exhibited slightly
393 different distributions. The PSD for El Chichón exhibited a distribution and volume
394 concentration similar to the background. However, the El Chichón PSD presented a
395 comparatively higher volume concentration in the finer particles (3.0-6.0 μm), not identified in
396 the background PSD. The PSD for Pinatubo/Hudson and 2001L present similar distributions
397 with volume concentrations up to an order of magnitude higher than the background. Despite
398 their similarities, the PSD for Pinatubo/Hudson displays a sharp decrease after reaching its
399 highest particle diameter (D) value at D=6 μm, while the PSD for 2001L reaches a steady
400 volume concentration value after D=8 μm. The mode particle diameters for Pinatubo/Hudson
401 (1991 AD) and El Chichón (1982 AD) matched the mode particle diameter of the background (6
402 μm). Unlike the other targeted horizons, the 2001L presented a higher mode particle diameter (8
403 μm).

404 ### 3.3.3 Microscopy analyses

405 Two filters containing insoluble particulate material from the 2001L of JUR were
406 analysed for microparticle characterization (Figure 6e). Seventy particles were identified as
407 cryptotephra shards with a mean size of 19.28 ± 8.73 μm (sizes ranging from 7 to 47 μm).
408 Similarly, two filters containing insoluble particulate matter from the 2001L of GOM were
409 analysed. Ten particles were identified as cryptotephra shards (Figure 6f) with a mean size of

12.9 ± 3.9 µm (sizes ranging from 7 to 20 µm). Most of the cryptotephra shards identified in both sites (JUR and GOM) were characterized by angular morphologies and concave features (vesicles) without evidence of alteration or corrosion. The cryptotephra shards are cuspate, platy with sharp edges and few with open vesicles and some with butterfly shape. Microscope slides from the 2001L of JUR show ten cryptotephra shards with a mean size of 21 µm and presented platy and cuspate textures with round vesicles (Figure 6g).

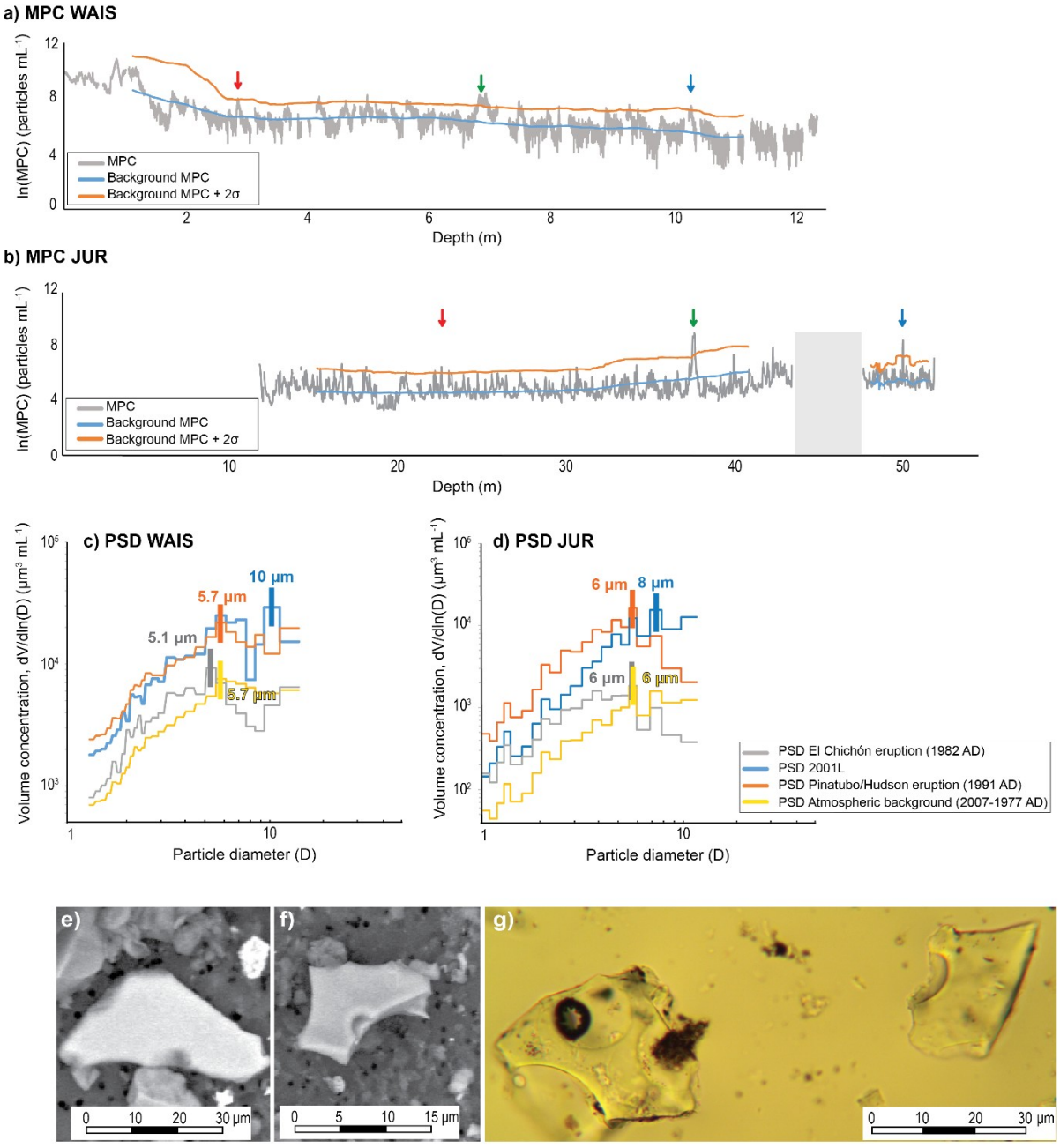

Figure 6. Microparticle analyses from WAIS and JUR ice cores. a) MPC for the depth interval corresponding to the 1977-2007 AD period from the WAIS ice core. b) MPC for the depth interval corresponding to the 1977-2007 AD period from the Jurassic ice core. Red arrows indicate peaks above the detection threshold in the 2001 AD ice core layer. Green arrows

indicate peaks above the detection threshold in the 1994-1992 AD ice core layer. Blue arrows indicate peaks above the detection threshold in the 1984-1982 AD ice core layer. The grey band indicates a gap in the dust record. c) PSD curves from the WAIS ice core. d) PSD curves from the Jurassic ice core. e) and f) show SEM micrographs of cryptotephra shards identified in the 2001 ice core layer from JUR and GOM ice cores respectively. g) Light microscope micrograph of cryptotephra shards identified in the 2001 AD ice core layer from Jurassic ice core.

3.4 Air mass trajectories

Forward trajectory analyses showed most of the air masses passing over the Balleny Islands on the 12th of June 2011 remained within the Southern Ocean for several days, mainly over the Somov, Ross, Amundsen and Bellingshausen Seas (Figure 7). Trajectories show air masses were predominantly travelling over the June sea-ice zone, with short periods (<72 hrs) of transit either over the Antarctic coast (<1000 m a.s.l) or over the ice sheet (>1000 m a.s.l.). After leaving the Balleny Islands, all air masses moving at 1000 m a.s.l. transited over the Oates Coast, some of them reaching Saunders Coast in Marie Byrd Land (See Figure 1 for geographical references). A similar pattern is present in air masses moving at 1500 m a.s.l., where most trajectories transit over the same regions, but some also reach the Walgreen Coast, next to the Amundsen Sea Embayment. Trajectories over 2000 m a.s.l. present a different pattern with most trajectories moving north towards lower latitudes and only some of them travelling back south and over the ice sheet in Marie Byrd Land, Ellsworth Land and the southern Antarctic Peninsula. These trajectories passing over Ellsworth Land and the southern Antarctic Peninsula are the only trajectories reaching the ice core sites (GOM, JUR, BC, 01-4). These five trajectories represent the paths followed by air masses passing over the Balleny Islands at: 1200, 1300, 1400, 2300 UTC on the 12th June 2011 and at 0200 UTC on the 13th June 2001. After leaving the Balleny Islands, four of these trajectories (1200, 1300, 1400 and 2300 UTC) were transported E-NE and then North, leaving the Southern Ocean and reaching ~ 43°S. Then they were transported back over the Southern Ocean southwards to the continent. The 0200 UTC trajectory remained within the June sea-ice zone and then over the ice sheet in Ellsworth Land and the southern Antarctic Peninsula. An additional cluster of five trajectories was identified passing near WAIS and 01-4 ice core sites at 1500 m a.s.l. These trajectories were passing over the Balleny Islands between 0800-1300 UTC on the 12th June 2001. After leaving the Balleny Islands they were transported over the June sea-ice zone of the Amundsen Sea and then reached the Walgreen Coast in the Amundsen Sea embayment.

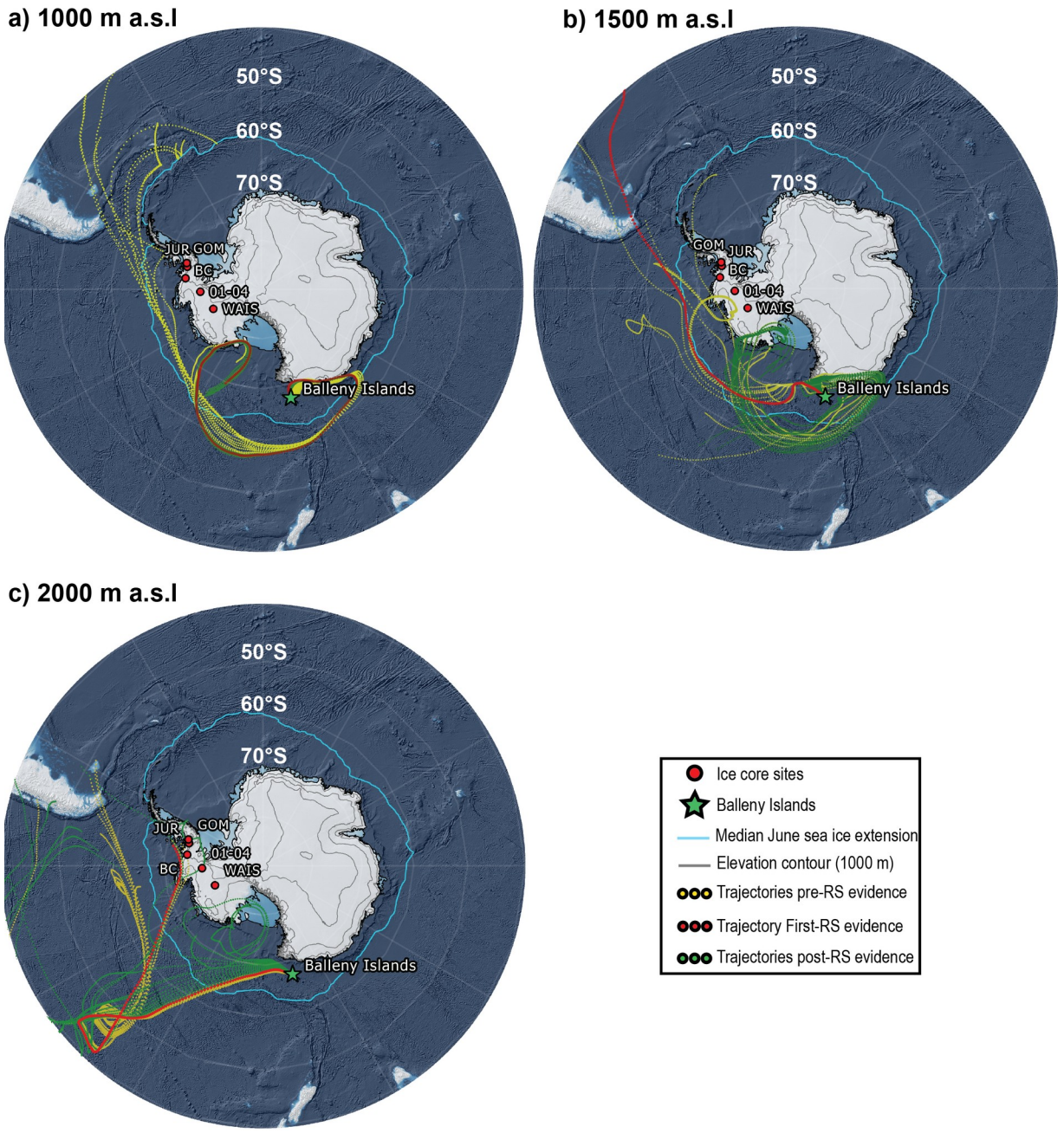

Figure 7. Trajectories departing from Sturge Island on the 12th of June 2001 at three different heights: a) 1000, b) 1500 and c) 2000 m a.s.l. Colour coded trajectories indicate if they passed through Sturge Island before, during or after the first remote sensing evidence of an unusual cloud formation. Median June sea ice-extension is based on 1980-2010 AD

4 Discussion

4.1 Pinatubo/Hudson (1991 AD) and El Chichón (1982 AD) eruptions

The 1994-1992 AD and 1984-1982 AD ice core layers are distinctive periods in the ice core record. These intervals show strong similarities in the presence and consistency of prominent summer peaks above the background variability in total sulphate concentration

463 (SO_4^{2-}), Electrical Conductivity (EC) and Microparticle concentration (MPC). The levels of SO_4^{2-}
464 and MPC in the two are above the detection threshold, suggesting an additional input of SO_4^{2-}
465 and microparticles during these periods. In Antarctica, the 1994-1992 AD and 1984-1982 AD ice
466 core layers have been linked to the well-documented eruptions of Mount Pinatubo/Cerro Hudson
467 (1991 AD)(Cole-Dai & Mosley-Thompson, 1999; Zhang et al., 2002; Jiang et al., 2012;
468 Plummer et al., 2012; Osipov et al., 2014; Schwanck et al., 2017; Thoen et al., 2018; Hoffmann
469 et al., 2020) and El Chichón (1982 AD)(Kohno et al., 1999; Traufetter et al., 2004; Jiang et al.,
470 2012; Plummer et al., 2012; Inoue et al., 2017; Thoen et al., 2018), the two volcanic eruptions
471 with the greatest SO_2 emissions worldwide of the 1977-2007 AD period (Shinohara, 2008).
472 Therefore, we propose the excess of SO_4^{2-} and microparticles identified during these periods
473 (1994-1992 AD & 1984-1982 AD) were also derived from the large low-latitude (mid-latitude)
474 Pinatubo (Cerro Hudson) and El Chichón eruptions.

475 Subtle differences were identified between the signals of SO_4^{2-}, nss SO_4^{2-}, EC and MPC
476 from the 1994-1992 AD and 1984-1982 AD ice core layers. The principal difference was
477 associated with the magnitude of the SO_4^{2-}, nss SO_4^{2-}, EC and MPC peak(s) in each layer. Peaks
478 in the 1994-1992 AD ice core layer were higher and more persistent, while peaks from the 1984-
479 1982 AD ice layer were smaller or absent (nssSO_4^{2-}-flux). These discrepancies are explained by
480 differences in the volumetric emissions from each eruption, classified on the logarithmic scale of
481 the Volcanic Explosivity Index (VEI). As VEI-6 (VEI-5), the Pinatubo (Cerro Hudson) eruption
482 released at least 10 km^3 (1 km^3) of particles and gases to the atmosphere, whilst the El Chichón
483 VEI-5 eruption, ejected only 1 km^3. The difference in the scale of these two eruptions accounts
484 for the different signal strengths observed in the 1994-1992 and 1984-1982 AD ice layers. Our
485 results are consistent with observations from several Antarctic ice cores presenting a stronger
486 signal for Pinatubo/Hudson and a weaker signal for El Chichón (Plummer et al., 2012; Inoue et
487 al., 2017; Thoen et al., 2018).

488 The records identified for the Pinatubo/Hudson and El Chichón eruptions provide two
489 examples of how different parameters measured in ice cores from the southern Antarctic
490 Peninsula, Ellsworth Land and Marie Byrd Land can effectively record recent major low-latitude
491 volcanic eruptions.

492 4.2 The 2001 AD ice core horizon

493 In 2001, remote sensing observations from Sturge Island presented inconclusive evidence
494 for recent volcanic activity in the Balleny Islands. Numerous lines of evidence from the ice core
495 record provide independent evidence that a high-latitude volcanic eruption occurred at this time.

496 The 2001 ice core layer (2001L) presents some of the most striking features identified in
497 the 1977-2007 AD period. In particular, this layer exhibited a prominent and synchronous SO_4^{2-}-
498 EC>2σ-peak on each ice core analysed. Its presence in ice across Marie Byrd Land, Ellsworth
499 Land and the southern Antarctic Peninsula, highlights it as a persistent regional feature. Even
500 though the >2σ signal is only represented by a single data point in two ice core records (SO_4^{2-} in
501 JUR and WAIS), its consistent presence across the region rules out the possibility of analytical
502 outliers or sample contamination. The magnitude and regional distribution of the SO_4^{2-}-EC>2σ-
503 peaks suggest it was caused by an exceptional input of sulphates to an extended area of the ice
504 sheet during mid-2001. Further analyses of the MSA record showed the absence of peaks during
505 the austral autumn/winter of 2001. Thus, demonstrating the SO_4^{2-}-EC>2σ-peak was not produced
506 by increased austral autumn/winter marine biogenic productivity. The lack of evidence for a

biogenic source suggests the SO_4^{2-}>2σ-peak identified in the 2001 ice core layer could only have been caused by inputs from a volcanic source. Detection of numerous cryptotephra glass shards in the mid-2001 AD ice core layer from the JUR and GOM ice cores provides direct evidence for a volcanic eruption. Combined with the observed MPC>2σ-peak in WAIS and JUR for the 2001L, this supports the assertion that the excess SO_4^{2-} is derived from a volcanic source. The elevated inputs of SO_4^{2-} & MPC recorded in 2001L are comparable to those observed in the 1994-1992 AD and 1984-1982 AD ice core layers, attributed to Pinatubo/Hudson and El Chichón eruptions, respectively (section 4.1).

Results from Particle Size Distribution (PSD) analyses spatially constrain a possible source for the 2001 volcanic products. In particular, the PSD profile for the 2001 MPC>2σ-peak presented a considerable increase in the volume and size of particles (mode diameter = 10 μm), compared with the background PSD (mode diameter = 5.7 μm). The coarser-than background PSD in 2001L suggest a more proximal volcanic source (Koffman et al., 2013) because coarser particles are unlikely to be transported large distances. Additionally, the spatial gradient identified in the volcanic sulphate flux suggests the transport and deposition of volcanic sulphate was from the Amundsen Sea sector towards the Bellingshausen Sea sector. Thus, establishing an eastward dispersion of the volcanic cloud. Results from the PSD and the net volcanic sulphate fluxes (VSF) are complemented by the synchronous deposition of the SO_4^{2-}, EC and MPC peaks that indicate rapid tropospheric transport and therefore also support a closer volcanic source (Koffman et al., 2017). Similarly, the angular texture of the cryptotephras suggest these glass shards were produced, transported and deposited within a short interval, without being altered by reworking or weathering processes.

To date, the Global Volcanic Program list of volcanic emissions only record two major volcanic events (VEI≥4) for the 1998-2001 AD period. These events correspond to Shiveluch volcano in Russia (ongoing eruption since 1999 AD, VEI=4) and to Ulawun volcano in Papua New Guinea (September 2000 AD, VEI=4). Additionally, during the same period, there is only one confirmed major source of SO_2 volcanic emissions, the Nyamuragira volcano in equatorial Africa (Shinohara, 2008). In the 1998-2001 AD period, the Nyamuragira volcano erupted three times: October 1998 AD, January 2000 AD and February 2001 AD. All these eruptions presenting a VEI=2. Despite the evidence of two major volcanic events and considerable SO_2 volcanic emissions from Nyamuragira during the 1998-2001 AD period, all these events occurred either in the equatorial region or in the northern hemisphere mid-latitudes. The distant location of these eruptions, their magnitude (VEI≤4) and their timing cannot explain the synchronous SO_4^{2-}, EC and MPC peaks or the presence of cryptotephra shards in the 2001L. Thus, establishing a small to moderate Antarctic eruption as the potential source of volcanic products present in the 2001 ice core layer.

Mount Erebus has been volcanically active since 1972 AD and is the only volcano listed to have recorded volcanic activity in Antarctica between 1998-2001 AD. The eruptions recorded during this period were of Strombolian type and not exceeding VEI=2. There was a substantial increase in the number of eruptions per month during 1998 AD and 2000 AD. However, there was a sharp decrease in the number of eruptions after May 2000 AD, leading to the absence of eruptions between March 2001 and February 2002 (Global Volcanism Program, 2006, Global Volcanism Program, 2017). Despite the potential of Mount Erebus to be considered as the source to the volcanic signature in the 2001L, the relatively continuous emission from small eruptions would be represented in the ice core record as the background signal, rather than as prominent

peaks. Moreover, the proximity of Mount Erebus to the ice core sites would require a small to moderate eruption to have occurred in mid-2001. However, the lack of eruptions during this period rules out the possibility of Erebus as the source of volcanic products seen in the 2001 ice core layer. Although Mount Erebus is discarded as the volcanic source, a potential small to moderate Antarctic eruption is consistent with remote sensing observations from Sturge Island on the 12th of June 2001.

The analyses of air mass transport pathways provide key evidence linking remote sensing observations to the ice core record. Trajectory analyses confirm air parcels passing over Sturge Island at low elevations (1500 and 2000 m a.s.l) during the unusual cloud formation, were transported to the ice core sites in Ellsworth Land and southern Antarctic Peninsula within a week. The detection of a volcanic signal in the WAIS ice core, despite trajectories not passing directly over the ice core site, can be explained by the coarse resolution of the trajectory model (2.5 degrees lat.-long.), potential mixing with neighbouring air parcels (both vertically and horizontally), and/or trajectories reaching the site after the designated 10-day period. The air masses passing over Sturge Island on the 12th of June 2001, likely incorporated particles and chemical compounds from the eruption cloud then carried and deposited them over Marie Byrd Land, Ellsworth Land and the southern Antarctic Peninsula.

Results presented here are consistent with previous studies identifying the Balleny Islands as the source of earlier volcanic products preserved in the ice core record from Marie Byrd Land (Dunbar et al., 2003; Kurbatov et al., 2006; Koffman et al., 2013). In particular, Buckle Island is suggested as the source of three cryptotephra layers deposited on 1839 AD, 1809 AD and 1804 AD (Kurbatov et al., 2006). The most recent of which was confirmed by historical records from sailors who observed a volcanic plume rising from Buckle Island in 1839 AD (LeMasurier et al., 1990). This 1839 eruption was recognized in the WAIS ice core and characterized by the presence of cryptotephra in two horizons with elevated particle concentration and a considerable increase of the mode particle diameter (>10 μm) over the PSD background dust (5.1 μm) (Koffman et al., 2013). Likewise, several cryptotephra layers identified in the ice core record show that Antarctic eruptions typically increase the mode particle diameter (>6 μm) (Narcisi et al., 2010; Koffman et al., 2013) corresponding with elevated SO_4^{2-}-EC and MPC deposition. In addition, air mass trajectories are consistent with previous studies showing the absence of a 2001 Sturge Island eruption record in ice cores from the inland sites of Mount Johns and the Ellsworth Mountains in the West Antarctic ice sheet (Thoen et al., 2018; Hoffmann et al., 2020).

In summary, the ice core records, air mass trajectory analyses and remote sensing observations presented here provide strong evidence that a short-lived, small to moderate volcanic eruption took place on Sturge Island in mid-2001. Evidence suggests that volcanic products from this eruption were rapidly transported through the troposphere and deposited inland over Marie Byrd Land, Ellsworth Land and the southern Antarctic Peninsula. The deposition over the ice sheet produced a volcanically enriched layer that has been preserved in the ice core record.

The detection of this 2001 eruption demonstrates Sturge Island is an active volcano capable of producing small-moderate explosive events. It is possible that previous eruptions recognised in Antarctic ice core records and attributed to Buckle Island, could instead, have originated from Sturge Island. If true, Sturge Island could be at least as active as Buckle Island. Thus, suggesting a reinterpretation of the Balleny Island hot-spot dynamics (Green, 1992).

Additionally, the prominent and consistent volcanic signal identified in the 2001 ice core layers from Marie Byrd Land, Ellsworth Land and the southern Antarctic Peninsula highlight this ice core horizon as a new, XXI century, chronostratigraphic marker between the eruptions of Pinatubo/Hudson (1991 AD, VEI=6 and VEI=5) and Puyehue-Cordon Caulle (2011 AD, VEI=5). As such, the Sturge Island 2001 eruption provides a valuable volcanic horizon to date ice cores from the Amundsen and Bellingshausen Seas sectors.

The evidence presented in this work of a new XXI century volcanic horizon in West Antarctic ice cores supports the occurrence of a volcanic eruption in Sturge Island in 2001. Whilst, geochemical analyses of the cryptotephra shards would be required to unequivocally determine the Balleny Islands as the volcanic source, the evidence presented here is sufficiently robust to assign this cryptotephra layer in ice cores as a chronostratigraphic marker.

5 Conclusions

Antarctica is one of the most uncertainly active volcanic regions on Earth, with hundreds of volcanoes hidden beneath the ice sheet. New historical records of active volcanism in Antarctica provide valuable information to study how volcanic activity can shape the polar climate and its potential impacts on the cryosphere. A set of ice core records from Marie Byrd Land, Ellsworth Land and the southern Antarctic Peninsula have been analysed to validate previous inconclusive evidence of a 2001 volcanic eruption on Sturge Island, part of the Balleny Island chain. The 2001 ice core layer contains a regional input of sulphates and microparticles consistent with a volcanic source. Particle coarsening and in-phase deposition of volcanic products evidenced a small to moderate Antarctic eruption as the source and a rapid tropospheric dispersion as the transport mechanism. Air mass trajectory analyses proved air parcels passing over Sturge Island during the 2001 eruption were effectively transported, within a week, to the ice core sites.

The evidence presented here builds on previous inconclusive remote sensing observations to advocate Sturge Island as an active volcano with recent eruptive states. The regional extent of this volcanic event across several Antarctic ice core records highlights it potential as a chronostratigraphic marker to improve the accuracy of 21st century ice chronologies. Further research should be focused on performing geochemical analyses of the cryptotephra shards to unequivocally fingerprint the volcanic source.

Acknowledgments

We would like to thank Christine Lane from the Geography Department, University of Cambridge, for her help with cryptotephra shard identification. We would like to thank Professor Eric Wolff from the Earth Sciences Department, University of Cambridge, for his comments and suggestions during the final reviewing and editing of this draft. Also, we would like to thank the Ice core Lab staff from the British Antarctic Survey, for their help while processing the Jurassic ice core. This research was funded by CONICYT–Becas Chile and Cambridge Trust funding program for PhD studies. Grant number 72180432.

Data Availability Statement

Datasets for this research are available in these in-text data citation references: Thomas et al., 2008; Thomas et al., 2015; Mayewski and Dixon, 2005; Sigl et al., 2016. WAIS Divide datasets are available at National Snow and Ice Data Center (https://nsidc.org/data/agdc/data-

wais-divide) and at the U.S. Antarctic Program Data Center (https://www.usap-dc.org/). Datasets from the ITASE 01-4 ice core are available at NASA Earth Data Common Metadata repository (https://cmr.earthdata.nasa.gov/search/concepts/C1214591464-SCIOPS). Datasets original to this work will be available at the UK Polar Data Center (https://www.bas.ac.uk/data/uk-pdc/).

Conflict of interest

The authors declare that the research was conducted in the absence of any commercial or financial relationships that could be construed as a potential conflict of interest.

References

Abram, N. J., Thomas, E. R., McConnell, J. R., Mulvaney, R., Bracegirdle, T. J., Sime, L. C., & Aristarain, A. J. (2010). Ice core evidence for a 20th century decline of sea ice in the Bellingshausen Sea, Antarctica. *Journal of Geophysical Research: Atmospheres*, *115*(D23).

Abram, N. J., Mulvaney, R., & Arrowsmith, C. (2011). Environmental signals in a highly resolved ice core from James Ross Island, Antarctica. *Journal of Geophysical Research: Atmospheres*, *116*(D20).

Abram, N. J., Mulvaney, R., Wolff, E. W., Triest, J., Kipfstuhl, S., Trusel, L. D., Vimeux, F., Fleet, L., & Arrowsmith, C. (2013). Acceleration of snow melt in an Antarctic Peninsula ice core during the twentieth century. Nature Geoscience, 6(5), 404–411. https://doi.org/10.1038/ngeo1787

Aristarain, A. J., & Delmas, R. J. (1998). Ice record of a large eruption of Deception Island Volcano (Antarctica) in the XVIIth century. *Journal of Volcanology and Geothermal Research*, *80*(1-2), 17-25.

Basile, I., Petit, J. R., Touron, S., Grousset, F. E., & Barkov, N. (2001). Volcanic layers in Antarctic (Vostok) ice cores: Source identification and atmospheric implications. *Journal of Geophysical Research: Atmospheres*, *106*(D23), 31915-31931.

Bingham, R. G., & Siegert, M. J. (2009). Quantifying subglacial bed roughness in Antarctica: implications for ice-sheet dynamics and history. *Quaternary Science Reviews*, *28*(3-4), 223-236.

Breton, D. J., Koffman, B. G., Kurbatov, A. V., Kreutz, K. J., & Hamilton, G. S. (2012). Quantifying signal dispersion in a hybrid ice core melting system. *Environmental science & technology*, *46*(21), 11922-11928.

Budner, D., & Cole-Dai, J. (2003). The number and magnitude of large explosive volcanic eruptions between 904 and 1865 AD: Quantitative evidence from a new South Pole ice core. *GEOPHYSICAL MONOGRAPH-AMERICAN GEOPHYSICAL UNION*, *139*, 165-176.

Castellano, E., Becagli, S., Jouzel, J., Migliori, A., Severi, M., Steffensen, J. P., Traversi, R., & Udisti, R. (2004). Volcanic eruption frequency over the last 45 ky as recorded in Epica-Dome C ice core (East Antarctica) and its relationship with climatic changes. Global and Planetary Change, 42(1–4), 195–205. https://doi.org/10.1016/j.gloplacha.2003.11.007

678 Cole−Dai, J., Mosley−Thompson, E., & Thompson, L. G. (1997). Annually resolved southern
679 hemisphere volcanic history from two Antarctic ice cores. *Journal of Geophysical*
680 *Research: Atmospheres*, *102*(D14), 16761-16771.

681 Cole-Dai, J., & Mosley-Thompson, E. (1999). The Pinatubo eruption in South Pole snow and its
682 potential value to ice-core paleovolcanic records. *Annals of Glaciology*, *29*, 99-105.

683 Cole−Dai, J., Mosley−Thompson, E., Wight, S. P., & Thompson, L. G. (2000). A 4100−year
684 record of explosive volcanism from an East Antarctica ice core. *Journal of Geophysical*
685 *Research: Atmospheres*, *105*(D19), 24431-24441.

686 Cole−Dai, J. (2010). Volcanoes and climate. *Wiley Interdisciplinary Reviews: Climate*
687 *Change*, *1*(6), 824-839.

688 Criscitiello, A. S., Das, S. B., Evans, M. J., Frey, K. E., Conway, H., Joughin, I., Medley, B., &
689 Steig, E. J. (2013). Ice sheet record of recent sea-ice behavior and polynya variability in
690 the Amundsen Sea, West Antarctica. Journal of Geophysical Research: Oceans, 118(1),
691 118–130. https://doi.org/10.1029/2012jc008077

692 Curran, M. A., van Ommen, T. D., Morgan, V. I., Phillips, K. L., & Palmer, A. S. (2003). Ice core
693 evidence for Antarctic sea ice decline since the 1950s. *Science*, *302*(5648), 1203-1206.

694 Dixon, D., Mayewski, P. A., Kaspari, S., Sneed, S., & Handley, M. (2004). A 200 year sub-
695 annual record of sulfate in West Antarctica, from 16 ice cores. *Annals of Glaciology*, *39*,
696 545-556.

697 Draxler, R. R., & Hess, G. D. (1998). An overview of the HYSPLIT_4 modelling system for
698 trajectories. *Australian meteorological magazine*, *47*(4), 295-308.

699 Dunbar, N. W., Zielinski, G. A., & Voisins, D. T. (2003). Tephra layers in the Siple Dome and
700 Taylor Dome ice cores, Antarctica: Sources and correlations. *Journal of Geophysical*
701 *Research: Solid Earth*, *108*(B8).

702 Dunbar, N. W., & Kurbatov, A. V. (2011). Tephrochronology of the Siple Dome ice core, West
703 Antarctica: correlations and sources. *Quaternary Science Reviews*, *30*(13-14), 1602-1614.

704 de Vries, M. V. W., Bingham, R. G., & Hein, A. S. (2018). A new volcanic province: an
705 inventory of subglacial volcanoes in West Antarctica. Geological Society, London,
706 Special Publications, 461(1), 231-248.

707 Fujita, S., Parrenin, F., Severi, M., Motoyama, H., & Wolff, E. W. (2015). Volcanic
708 synchronization of Dome Fuji and Dome C Antarctic deep ice cores over the past 216
709 kyr. *Climate of the Past*, *11*(10), 1395-1416.

710 Gautier, E., Savarino, J., Erbland, J., Lanciki, A., & Possenti, P. (2016). Variability of sulfate
711 signal in ice core records based on five replicate cores. *Climate of the Past*, *12*(1), 103-
712 113.

713 Global Volcanism Program, 2001. Report on Sturge Island (Antarctica) (Wunderman, R.,
714 ed.). *Bulletin of the Global Volcanism Network*, 26:5. Smithsonian Institution.
715 https://doi.org/10.5479/si.GVP.BGVN200105-390012

Global Volcanism Program, 2006. Report on Erebus (Antarctica) (Wunderman, R., ed.). Bulletin of the Global Volcanism Network, 31:12. Smithsonian Institution. https://doi.org/10.5479/si.GVP.BGVN200612-390020.

Global Volcanism Program, 2017. Report on Erebus (Antarctica) (Crafford, A.E., and Venzke, E., eds.). Bulletin of the Global Volcanism Network, 42:6. Smithsonian Institution. https://doi.org/10.5479/si.GVP.BGVN201706-390020.

Goodwin, B. P. (2013). *Recent Environmental Changes on the Antarctic Peninsula as Recorded in an ice core from the Bruce Plateau* (Doctoral dissertation, The Ohio State University).

Green, T. H. (1992). Petrology and geochemistry of basaltic rocks from the Balleny Is, Antarctica. *Australian Journal of Earth Sciences*, *39*(5), 603-617.

Hoffmann, K., Fernandoy, F., Meyer, H., Thomas, E. R., Aliaga, M., Tetzner, D., Freitag, J., Opel, T., Arigony-Neto, J., Göbel, C. F., Jaña, R., Rodríguez Oroz, D., Tuckwell, R., Ludlow, E., McConnell, J. R., & Schneider, C. (2020). Stable water isotopes and accumulation rates in the Union Glacier region, Ellsworth Mountains, West Antarctica, over the last 35 years. The Cryosphere, 14(3), 881–904. https://doi.org/10.5194/tc-14-881-2020

Hund, A. J. (Ed.). (2014). Antarctica and the Arctic Circle: A Geographic Encyclopedia of the Earth's Polar Regions [2 volumes]. ABC-CLIO.

Inoue, M., Curran, M. A., Moy, A. D., van Ommen, T. D., Fraser, A. D., Phillips, H. E., & Goodwin, I. D. (2017). A glaciochemical study of the 120 m ice core from Mill Island, East Antarctica. *Climate of the Past*, *13*(5), 437-453.

Jiang, S., Cole-Dai, J., Li, Y., Ferris, D. G., Ma, H., An, C., Shi, G., & Sun, B. (2012). A detailed 2840 year record of explosive volcanism in a shallow ice core from Dome A, East Antarctica. Journal of Glaciology, 58(207), 65–75. https://doi.org/10.3189/2012jog11j138

JIANKANG, H., ZICHU, X., JIAHONG, W., JIANCHENG, K., & GUOCAI, Z. (1999). Mass balance study on Collins Ice Cap, King George Island, Antarctica: spatial and temporal variations. *IAHS-AISH publication*, 209-215.

Kittleman, L. R. (1979). Tephra. *Scientific American*, *241*(6), 160-177.

Koffman, B. G., Kreutz, K. J., Kurbatov, A. V., & Dunbar, N. W. (2013). Impact of known local and tropical volcanic eruptions of the past millennium on the WAIS Divide microparticle record. *Geophysical research letters*, *40*(17), 4712-4716.

Koffman, B. G., Kreutz, K. J., Breton, D. J., Kane, E. J., Winski, D. A., Birkel, S. D., Kurbatov, A. V., & Handley, M. J. (2014). Centennial-scale variability of the Southern Hemisphere westerly wind belt in the eastern Pacific over the past two millennia. Climate of the Past, 10(3), 1125–1144. https://doi.org/10.5194/cp-10-1125-2014

Koffman, B. G., Dowd, E. G., Osterberg, E. C., Ferris, D. G., Hartman, L. H., Wheatley, S. D., Kurbatov, A. V., Wong, G. J., Markle, B. R., Dunbar, N. W., Kreutz, K. J., & Yates, M. (2017). Rapid transport of ash and sulfate from the 2011 Puyehue-Cordón Caulle (Chile) eruption to West Antarctica. Journal of Geophysical Research: Atmospheres, 122(16), 8908–8920. https://doi.org/10.1002/2017jd026893

KOHNO, M., FUJII, Y., KUSAKABE, M., & FUKUOKA, T. (1999). The last 300-year volcanic signals recorded in an ice core from site H15, Antarctica. *Journal of the Japanese Society of Snow and Ice*, *61*(1), 13-24.

Kreutz, K. J., & Mayewski, P. A. (1999). Spatial variability of Antarctic surface snow glaciochemistry: implications for palaeoatmospheric circulation reconstructions. *Antarctic Science*, *11*(1), 105-118.

Kreutz, K. J., Kurbatov, A. V., Wells, M., & Mayewski, P. A. (2011). COLLABORATIVE RESEARCH: Microparticle/tephra analysis of the WAIS Divide ice core.

Kreutz, K. et al. (2015) "WAIS Divide Microparticle Concentration and Size Distribution, 0-2400 ka" U.S. Antarctic Program (USAP) Data Center. doi: https://doi.org/10.7265/N5KK98QZ.

Kurbatov, A. V., Zielinski, G. A., Dunbar, N. W., Mayewski, P. A., Meyerson, E. A., Sneed, S. B., & Taylor, K. C. (2006). A 12,000 year record of explosive volcanism in the Siple Dome Ice Core, West Antarctica. *Journal of Geophysical Research: Atmospheres*, *111*(D12).

Lee, J. E., Brook, E. J., Bertler, N. A. N., Buizert, C., Baisden, T., Blunier, T., Ciobanu, V. G., Conway, H., Dahl-Jensen, D., Fudge, T. J., Hindmarsh, R., Keller, E. D., Parrenin, F., Severinghaus, J. P., Vallelonga, P., Waddington, E. D., & Winstrup, M. (2020). An 83 000-year-old ice core from Roosevelt Island, Ross Sea, Antarctica. Climate of the Past, 16(5), 1691–1713. https://doi.org/10.5194/cp-16-1691-2020

Legrand, M., & Mayewski, P. (1997). Glaciochemistry of polar ice cores: A review. *Reviews of geophysics*, *35*(3), 219-243.

LeMasurier, W. E., Thomson, J. W., Baker, P. E., Kyle, P. R., Rowley, P. D., Smellie, J. L., & Verwoerd, W. J. (1990). Volcanoes of the Antarctic plate and Southern Ocean (Vol. 48). American Geophysical Union.

Li, C., Xiao, C., Hou, S., Ren, J., Ding, M., & Guo, R. (2012). Dating a 109.9 m ice core from Dome A (East Antarctica) with volcanic records and a firn densification model. *Science China Earth Sciences*, *55*(8), 1280-1288.

Maupetit, F., & Delmas, R. J. (1992). Chemical composition of falling snow at Dumont d'Urville, Antarctica. *Journal of atmospheric chemistry*, *14*(1-4), 31-42.

Mayewski, P. A. and D. A. Dixon. 2005. US International Trans Antarctic Scientific Expedition (US ITASE) glaciochemical data. Boulder, CO, USA: National Snow and Ice Data Center. Digital media.

Mulvaney, R., Abram, N. J., Hindmarsh, R. C. A., Arrowsmith, C., Fleet, L., Triest, J., Sime, L. C., Alemany, O., & Foord, S. (2012). Recent Antarctic Peninsula warming relative to Holocene climate and ice-shelf history. Nature, 489(7414), 141–144. https://doi.org/10.1038/nature11391

Mulvaney, R. (2013). ICE CORE METHODS | Conductivity Studies. In Encyclopedia of Quaternary Science (pp. 319–325). Elsevier. https://doi.org/10.1016/b978-0-444-53643-3.00311-3

Narcisi, B., Petit, J. R., Delmonte, B., Basile-Doelsch, I., & Maggi, V. (2005). Characteristics and sources of tephra layers in the EPICA-Dome C ice record (East Antarctica):

implications for past atmospheric circulation and ice core stratigraphic correlations. *Earth and Planetary Science Letters*, *239*(3-4), 253-265.

Narcisi, B., Petit, J. R., & Delmonte, B. (2010). Extended East Antarctic ice-core tephrostratigraphy. *Quaternary Science Reviews*, *29*(1-2), 21-27.

Narcisi, B., Petit, J. R., Delmonte, B., Scarchilli, C., & Stenni, B. (2012). A 16,000-yr tephra framework for the Antarctic ice sheet: a contribution from the new Talos Dome core. *Quaternary Science Reviews*, *49*, 52-63.

Narcisi, B., Petit, J. R., Langone, A., & Stenni, B. (2016). A new Eemian record of Antarctic tephra layers retrieved from the Talos Dome ice core (Northern Victoria Land). *Global and planetary Change*, *137*, 69-78.

Narcisi, B., Petit, J. R., Delmonte, B., Batanova, V., & Savarino, J. (2019). Multiple sources for tephra from AD 1259 volcanic signal in Antarctic ice cores. *Quaternary Science Reviews*, *210*, 164-174.

Nardin, R., Amore, A., Becagli, S., Caiazzo, L., Frezzotti, M., Severi, M., Stenni, B., & Traversi, R. (2020). Volcanic Fluxes Over the Last Millennium as Recorded in the Gv7 Ice Core (Northern Victoria Land, Antarctica). Geosciences, 10(1), 38. https://doi.org/10.3390/geosciences10010038

Osipov, E. Y., Khodzher, T. V., Golobokova, L. P., Onischuk, N. A., Lipenkov, V. Y., Ekaykin, A. A., Shibaev, Y. A., & Osipova, O. P. (2014). High-resolution 900 year volcanic and climatic record from the Vostok area, East Antarctica. The Cryosphere, 8(3), 843–851. https://doi.org/10.5194/tc-8-843-2014

Palais, J. M. (1985). Particle morphology, composition and associated ice chemistry of tephra layers in the Byrd ice core: Evidence for hydrovolcanic eruptions. *Annals of glaciology*, *7*, 42-48.

Parrenin, F., Barker, S., Blunier, T., Chappellaz, J., Jouzel, J., Landais, A., Masson-Delmotte, V., Schwander, J., & Veres, D. (2012). On the gas-ice depth difference (Δdepth) along the EPICA Dome C ice core. Climate of the Past, 8(4), 1239–1255. https://doi.org/10.5194/cp-8-1239-2012

Patrick, M. R., & Smellie, J. L. (2013). Synthesis A spaceborne inventory of volcanic activity in Antarctica and southern oceans, 2000-10. *Antarctic Science*, *25*(4), 475.

Plummer, C. T., Curran, M. A. J., van Ommen, T. D., Rasmussen, S. O., Moy, A. D., Vance, T. R., Clausen, H. B., Vinther, B. M., & Mayewski, P. A. (2012). An independently dated 2000-yr volcanic record from Law Dome, East Antarctica, including a new perspective on the dating of the 1450s CE eruption of Kuwae, Vanuatu. Climate of the Past, 8(6), 1929–1940. https://doi.org/10.5194/cp-8-1929-2012

Ren, J., Li, C., Hou, S., Xiao, C., Qin, D., Li, Y., & Ding, M. (2010). A 2680 year volcanic record from the DT−401 East Antarctic ice core. *Journal of Geophysical Research: Atmospheres*, *115*(D11).

Robock, A. (2000). Volcanic eruptions and climate. *Reviews of geophysics*, *38*(2), 191-219.

Röthlisberger, R., Bigler, M., Hutterli, M., Sommer, S., Stauffer, B., Junghans, H. G., & Wagenbach, D. (2000). Technique for continuous high-resolution analysis of trace substances in firn and ice cores. *Environmental Science & Technology*, *34*(2), 338-342.

Ruth, U., Wagenbach, D., Steffensen, J. P., & Bigler, M. (2003). Continuous record of microparticle concentration and size distribution in the central Greenland NGRIP ice core during the last glacial period. *Journal of Geophysical Research: Atmospheres*, *108*(D3).

Schwanck, F., Simões, J. C., Handley, M., Mayewski, P. A., Auger, J. D., Bernardo, R. T., & Aquino, F. E. (2017). A 125-year record of climate and chemistry variability at the Pine Island Glacier ice divide, Antarctica. *The Cryosphere*, *11*(4), 1537-1552.

Severi, M., Udisti, R., Becagli, S., Stenni, B., & Traversi, R. (2012). Volcanic synchronisation of the EPICA-DC and TALDICE ice cores for the last 42 kyr BP. *Climate of the Past*, *8*(2), 509-517.

Shinohara, H. (2008). Excess degassing from volcanoes and its role on eruptive and intrusive activity. *Reviews of Geophysics*, *46*(4).

Sigl, M., McConnell, J. R., Toohey, M., Curran, M., Das, S. B., Edwards, R., Isaksson, E., Kawamura, K., Kipfstuhl, S., Krüger, K., Layman, L., Maselli, O. J., Motizuki, Y., Motoyama, H., Pasteris, D. R., & Severi, M. (2014). Insights from Antarctica on volcanic forcing during the Common Era. Nature Climate Change, 4(8), 693–697. https://doi.org/10.1038/nclimate2293

Sigl, M., Fudge, T. J., Winstrup, M., Cole-Dai, J., Ferris, D., McConnell, J. R., Taylor, K. C., Welten, K. C., Woodruff, T. E., Adolphi, F., Bisiaux, M., Brook, E. J., Buizert, C., Caffee, M. W., Dunbar, N. W., Edwards, R., Geng, L., Iverson, N., Koffman, B., … Sowers, T. A. (2016). The WAIS Divide deep ice core WD2014 chronology – Part 2: Annual-layer counting (0–31 ka BP). Climate of the Past, 12(3), 769–786. https://doi.org/10.5194/cp-12-769-2016

Stein, A. F., Draxler, R. R., Rolph, G. D., Stunder, B. J., Cohen, M. D., & Ngan, F. (2015). NOAA's HYSPLIT atmospheric transport and dispersion modeling system. *Bulletin of the American Meteorological Society*, *96*(12), 2059-2077.

Tetzner, D., Thomas, E. R., Allen, C. S., & Wolff, E. W. (2021). A Refined Method to Analyze Insoluble Particulate Matter in Ice Cores, and Its Application to Diatom Sampling in the Antarctic Peninsula. *Frontiers in Earth Science*, *9*, 20.

Thoen, I. U., Simões, J. C., Lindau, F. G. L., & Sneed, S. B. (2018). Ionic content in an ice core from the West Antarctic Ice Sheet: 1882-2008 AD. *Brazilian Journal of Geology*, *48*(4), 853-865.

Thomas, E. R., Marshall, G. J., & McConnell, J. R. (2008). A doubling in snow accumulation in the western Antarctic Peninsula since 1850. *Geophysical research letters*, *35*(1).

Thomas, E. R., Hosking, J. S., Tuckwell, R. R., Warren, R. A., & Ludlow, E. C. (2015). Twentieth century increase in snowfall in coastal West Antarctica. *Geophysical Research Letters*, *42*(21), 9387-9393.

Thomas, E. R., & Abram, N. J. (2016). Ice core reconstruction of sea ice change in the Amundsen−Ross Seas since 1702 AD. *Geophysical Research Letters*, *43*(10), 5309-5317.

Traufetter, F., Oerter, H., Fischer, H., Weller, R., & Miller, H. (2004). Spatio-temporal variability in volcanic sulphate deposition over the past 2 kyr in snow pits and firn cores from Amundsenisen, Antarctica. *Journal of Glaciology*, *50*(168), 137-146.

Traversi, R., Becagli, S., Castellano, E., Migliori, A., Severi, M., & Udisti, R. (2002). High-resolution fast ion chromatography (FIC) measurements of chloride, nitrate and sulphate along the EPICA Dome C ice core. *Annals of Glaciology*, *35*, 291-298.

Udisti, R., Becagli, S., Castellano, E., Mulvaney, R., Schwander, J., Torcini, S., & Wolff, E. (2000). Holocene electrical and chemical measurements from the EPICA–Dome C ice core. *Annals of Glaciology*, *30*, 20-26.

Vogel, S. W., Tulaczyk, S., Carter, S., Renne, P., Turrin, B., & Grunow, A. (2006). Geologic constraints on the existence and distribution of West Antarctic subglacial volcanism. *Geophysical research letters*, *33*(23).

Wagenbach, D., Ducroz, F., Mulvaney, R., Keck, L., Minikin, A., Legrand, M., Hall, J. S., & Wolff, E. W. (1998). Sea-salt aerosol in coastal Antarctic regions. Journal of Geophysical Research: Atmospheres, 103(D9), 10961–10974. https://doi.org/10.1029/97jd01804

Zhang, M. J., Li, Z. Q., Xiao, C. D., Qin, D. H., Yang, H. A., Kang, J. C., & Li, J. (2002). A continuous 250-year record of volcanic activity from Princess Elizabeth Land, East Antarctica. *Antarctic Science*, *14*(1), 55.